JBC ARTICLE

Acetylation modulates the Fanconi anemia pathway by protecting FAAP20 from ubiquitin-mediated proteasomal degradation

Received for publication, July 21, 2020, and in revised form, August 4, 2020 Published, Papers in Press, August 6, 2020, DOI 10.1074/jbc.RA120.015288

Bhavika Nagareddy[1], **Arafat Khan**[1], **and Hyungjin Kim**[1,2,*]

From the [1]*Department of Pharmacological Sciences, State University of New York at Stony Brook, Stony Brook, New York, USA and the* [2]*Stony Brook Cancer Center, Renaissance School of Medicine at Stony Brook University, Stony Brook, New York, USA*

Edited by John M. Denu

Fanconi anemia (FA) is a chromosome instability syndrome of children caused by inherited mutations in one of FA genes, which together constitute a DNA interstrand cross-link (ICL) repair, or the FA pathway. Monoubiquitination of Fanconi anemia group D2 protein (FANCD2) by the multisubunit ubiquitin E3 ligase, the FA core complex, is an obligate step in activation of the FA pathway, and its activity needs to be tightly regulated. FAAP20 is a key structural component of the FA core complex, and regulated proteolysis of FAAP20 mediated by prolyl *cis-trans* isomerization and phosphorylation at a consensus phosphodegron motif is essential for preserving the integrity of the FA core complex, and thus FANCD2 monoubiquitination. However, how ubiquitin-dependent FAAP20 degradation is modulated to fine-tune FA pathway activation remains largely unknown. Here, we present evidence that FAAP20 is acetylated by the acetyltransferase p300/CBP on lysine 152, the key residue that when polyubiquitinated results in the degradation of FAAP20. Acetylation or mutation of the lysine residue stabilizes FAAP20 by preventing its ubiquitination, thereby protecting it from proteasome-dependent FAAP20 degradation. Consequently, disruption of the FAAP20 acetylation pathway impairs FANCD2 activation. Together, our study reveals a competition mechanism between ubiquitination and acetylation of a common lysine residue that controls FAAP20 stability and highlights a complex balancing between different posttranslational modifications as a way to refine the FA pathway signaling required for DNA ICL repair and genome stability.

The Fanconi anemia (FA) pathway is a DNA repair mechanism that mainly resolves DNA interstrand cross-links (ICLs), a formidable type of DNA lesion that prevents both DNA replication and transcription (1, 2). Inherited deficiency in this pathway causes a chromosomal instability syndrome in children known as FA, which is characterized by developmental abnormalities and progressive bone marrow failure (3). In addition, affected children are predisposed to a variety of cancers, including acute myelogenous leukemia and squamous cell carcinoma of the head and neck, suggesting that the FA pathway plays a role as an essential tumor suppressor mechanism that retrains genome instability (4).

Germline mutations in any one of the 22 known FA complementation groups (*FANCA* to *FANCW*) result in the clinical symptoms of FA. Mechanistically, these gene products work in a common DNA repair process to recognize DNA ICLs during DNA replication fork progression and initiate the signaling that recruits enzymes necessary for repairing the lesion (5). This involves monoubiquitination of FANCD2 in the FANCI–FANCD2 (ID) heterodimeric complex by the FA core complex, a multisubunit ubiquitin E3 ligase, and localization of the ID complex at an ICL-induced stalled replication fork (6, 7). FANCD2 monoubiquitin (FANCD2-Ub) in turn recruits SLX4/FANCP and its associated 3′-flap structure-specific endonuclease, the XPF/FANCQ-ERCC1 heterodimer, which incises and unhooks the DNA ICL (8, 9). The incision results in a replication-associated double-strand break, which is repaired by translesion DNA synthesis and homologous recombination (10). In this sense, FANCD2 monoubiquitination by the FA core complex is a prerequisite step that enables downstream enzymatic repair processes in response to DNA damage, hence controlling the FA core complex activity is critical for the commitment of FA pathway activation.

The FA core complex consists of at least 8 FA proteins, namely FANCA/B/C/E/F/G/L/M along with several ancillary factors (11). *In vitro* reconstitution experiments have established that the FA core complex is modular, consisting of FANCB–FANCL–FAAP100, FANCA–FANCG–FAAP20, and FANCC–FANCE–FANCF, along with FANCM–FAAP24–MHF1/2, which is required for damage recognition and DNA remodeling (12–15). Recent cryo-EM studies have revealed that the FA core complex constitutes an extended asymmetric dimer, which suggests a distinct and independent role for each catalytic module (16, 17). Although the subcomplex that contains the FANCL ubiquitin E3 ligase subunit is sufficient for monoubiquitinating FANCD2 *in vitro*, loss of individual subunits in the FA core complex abolishes FANCD2 monoubiquitination in cells, indicating that each module is essential for maintaining the functional integrity of the FA core complex.

Among the FA core auxiliary proteins, FAAP20 (FA-associated protein, 20 kDa) constitutes a key regulatory protein that preserves the integrity of the FA core complex, and in our previous investigations, we have elucidated players and mechanisms that control the FA pathway via modulation of FAAP20 proteolysis (Fig. 1*A*). FAAP20 directly interacts with FANCA, a scaffold of the FA core complex, and they exist as an obligate

This article contains supporting information.

* For correspondence: Hyungjin Kim, hyungjin.kim@stonybrook.edu.

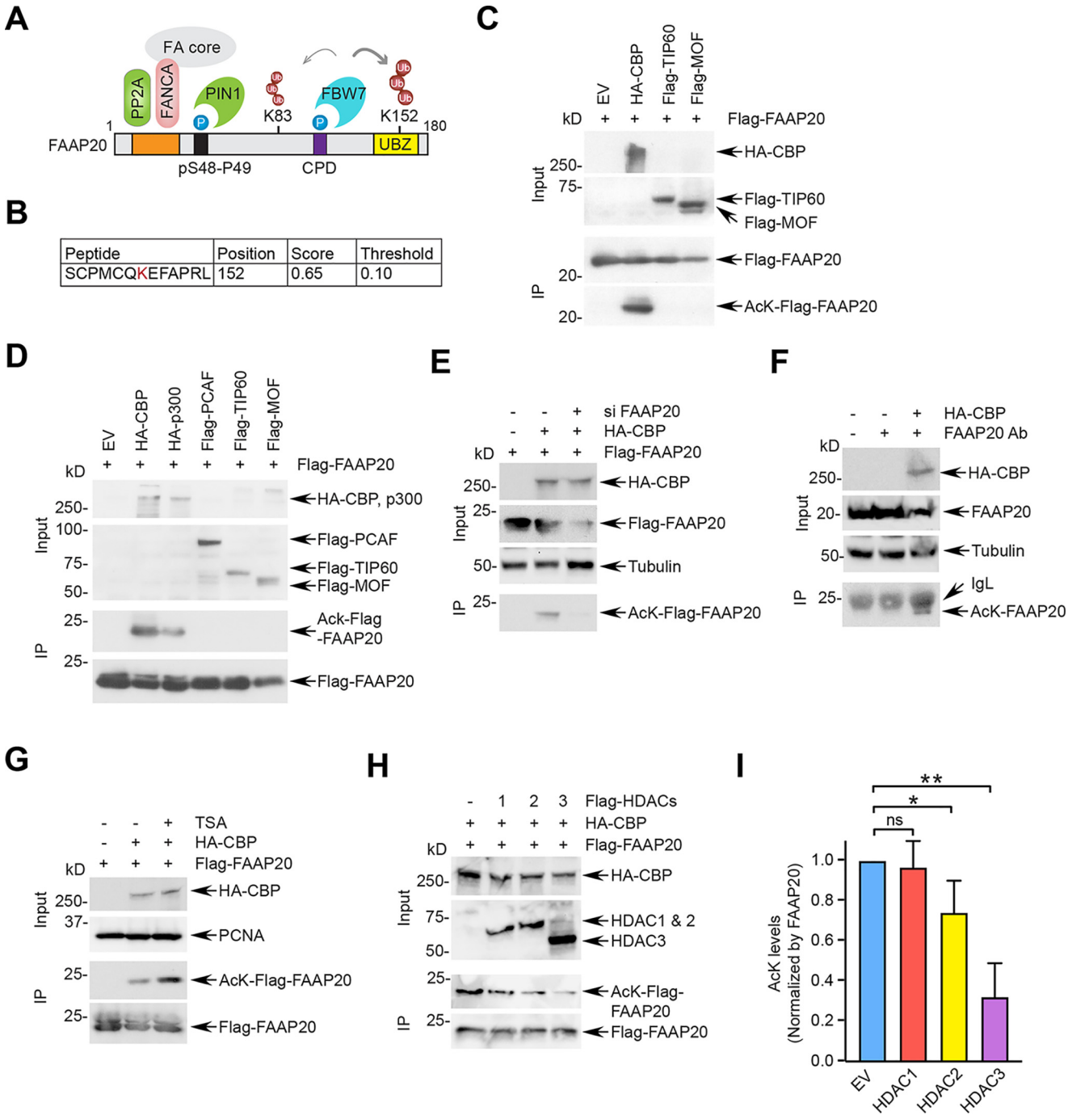

Figure 1. FAAP20 is acetylated by CBP/p300 and deacetylated by HDAC3. *A*, schematic of protein interaction networks that control FAAP20 proteolysis and function. Lys-152, a major site for ubiquitination within the ubiquitin-binding zinc finger (*UBZ*) is indicated. *pS48-P49*, phosphorylated PIN1 recognition site. *CPD*, Cdc4 phosphodegron. *B*, prediction outcome of the FAAP20 acetylation site at Lys-152 using PAIL (prediction of acetylation on internal lysines). *C* and *D*, screening of FAAP20 acetylation by multiple KATs. 293T cells expressing Flag–FAAP20 were transfected with the indicated KATs, and cell lysates were subjected to anti-Flag immunoprecipitation (*IP*), followed by Western blotting (*WB*) using an acetyl-Lys–specific antibody. *EV*, empty vector control. *E*, specificity of FAAP20 acetylation. 293T cells transfected with siRNA FAAP20 (*versus* control) were co-transfected with Flag–FAAP20 and HA–CBP, followed by anti-Flag IP and Western blot. *F*, acetylation of endogenous FAAP20. Cell lysates from 293T cells transfected with HA-CBP (*versus* EV) were immunoprecipitated by an anti-FAAP20 antibody (*versus* rabbit IgG control) and analyzed by Western blot. *G*, inhibition of FAAP20 deacetylation by TSA. 293T cells transfected with the indicated plasmids were left untreated or treated with 400 nM TSA for 16 h, and FAAP20 acetylation was analyzed by anti-Flag IP and Western blot. *H*, FAAP20 deacetylation by HDACs. 293T cells transfected with the indicated plasmids were subjected to anti-Flag IP and Western blot analysis. *I*, quantification of FAAP20 acetylation levels in *H*. *Error bar* indicates mean ± S.D., $n = 3$ from three independent experiments, **, $p < 0.01$; *, $p < 0.05$; *ns*, not significant, Student's *t* test.

heterodimer that is responsible for stabilizing each other (18–20). The N terminus of FAAP20 is required for interacting with FANCA to prevent proteasomal degradation of FANCA, and deficiency of FAAP20 leads to uncontrolled degradation of FANCA, mediated by SUMO-targeted ubiquitination of FANCA by RING finger protein 4 (RNF4) (21). Consequently,

FAAP20 depletion impairs FANCD2 monoubiquitination and subsequent resolution of DNA ICLs because the structural integrity of the FA core complex is compromised, thereby leading to the loss of its functionality. FAAP20 degradation is mediated by the multimeric SKP1–CUL1–F-Box (SCF)^{FBW7} ubiquitin E3 ligase complex, which recognizes the Cdc4 phosphodegron (CPD) motif that is phosphorylated by glycogen synthase kinase 3β to trigger FAAP20 polyubiquitination (22). Two lysine residues of FAAP20, Lys-83 and Lys-152, are the sites of SCF^{FBW7}-dependent polyubiquitination, among which Lys-152 has been shown to be a major modification site (22). Defective CPD phosphorylation increases cellular FAAP20 levels and prevents completion of DNA ICL repair, indicating that regulated FAAP20 turnover at sites of DNA damage, controlled by the CPD phosphorylation, is critical for completing the FA pathway. Furthermore, CPD phosphorylation status is regulated by phosphorylation-dependent *cis-trans* prolyl isomerization of FAAP20 near the N-terminal FANCA-interacting region, which is catalyzed by the PIN1 isomerase to promote FAAP20 stability (23). Mechanistically, the PIN1-induced structural change of FAAP20 enhances its interaction with the PP2A phosphatase, which removes the phosphate group from the CPD and thus counteracts FAAP20 degradation. This unique method of regulation highlights the role of dynamic protein–protein interactions and posttranslational modifications within the FA core complex for preserving its structural integrity and function. In this sense, it is not surprising to note that the individual FA core complex subunits are subjected to multiple posttranslational modifications both during the cell cycle and upon DNA damage (24). Nevertheless, it remains unclear how the ubiquitination levels of FAAP20 are adjusted to control the kinetics of FAAP20 degradation, which would impact the function of the FA core complex and dictate FA pathway activation.

Here, we reveal lysine acetylation as an additional posttranslational modification that controls FAAP20 stability. By sharing a common lysine for modification, acetylation of FAAP20 enhances its stability by interfering with FAAP20 ubiquitination and proteasomal degradation. This study identifies a mechanism whereby FA pathway signaling is controlled by a competition between ubiquitination and acetylation, and thus highlights the role of multiple posttranslational modifications in regulating the activity of the FA core complex and FANCD2 activation.

Results

FAAP20 is acetylated by p300/CBP and deacetylated by HDAC3

Because FAAP20 is subjected to multiple posttranslational modifications, we sought to identify additional modifications that may control the activity and stability of FAAP20. Interestingly, analysis of FAAP20 modifications via various prediction tools revealed that FAAP20 contains a potential acetylation site at Lys-152 (25)(Fig. 1*B*). This residue has been reported as a putative site for acetylation from a large-scale quantitative proteomic analysis, implying that endogenous FAAP20 may be regulated by acetylation (26). Protein acetylation on a lysine residue is a prevalent covalent modification in eukaryotes that modulates various properties of proteins, including protein interactions, stability, activity, and subcellular localization (27). Acetyl groups are added by lysine acetyltransferases (KATs), which transfer acetyl groups from acetyl-CoA to the ϵ-amino group of an internal lysine. This reversible process is balanced by lysine/histone deacetylases (HDACs), which remove acetyl groups and therefore antagonize KAT activity (28, 29).

To address whether FAAP20 is acetylated in the cells, we co-expressed Flag-tagged FAAP20 with various Flag- or HA-tagged KATs, followed by anti-Flag immunoprecipitation to specifically enrich exogenous Flag-FAAP20 (Fig. S1*A* for comparison between endogenous and exogenous FAAP20 expression). Immunoblot analysis using a pan-acetyl lysine antibody revealed that Flag–FAAP20 is acetylated by the p300/CBP (CREB-binding protein) family protein CBP (Fig. 1*C*). Both CBP (KAT3A) and its paralog p300 (KAT3B) belong to the KAT3 family, a group of enzymes that cooperatively bind and modify histones, as well as other nonhistone nuclear proteins that are involved in DNA replication and repair processes (30). Indeed, both CBP and p300 were able to induce FAAP20 acetylation (Fig. 1*D*). In contrast, other KAT family proteins, such as the MYST family TIP60 (KAT5) and MOF (KAT8), or the GNAT family PCAF (KAT2B) failed to do so, suggesting that the p300/CBP KAT3 proteins are responsible for FAAP20 acetylation in cells (Fig. 1, *C* and *D*). Additionally, knockdown of FAAP20 resulted in a decreased signal in the pan-acetyl lysine immunoblot induced by CBP expression, confirming the specificity of acetylation on FAAP20 (Fig. 1*E*). We were also able to detect acetylation of endogenous FAAP20 when CBP is exogenous expressed and FAAP20 was enriched by anti-FAAP20 immunoprecipitation (Fig. 1*F*). To further confirm the FAAP20 acetylation promoted by the p300/CBP acetyltransferases, we determined whether p300 and CBP are required for FAAP20 acetylation. To this end, we knocked down both p300 and CBP by previously validated siRNA oligonucleotides and confirmed its functionality by RT-quantitative PCR and Western blotting (31) (Fig. S1*B*). Anti-FAAP20 immunoprecipitation revealed that depletion of p300 and CBP results in disappearance of the FAAP20 acetylation signal, indicating that endogenous FAAP20 acetylation is controlled by p300 and CBP (Fig. S1*C*).

Notably, FAAP20 acetylation was preserved and enhanced when cells were pretreated with an HDAC inhibitor, trichostatin A (TSA), indicating that FAAP20 acetylation is antagonized by HDAC activity (Fig. 1*G*). TSA is known to target the class I and II HDAC family of enzymes, which include Zn^{2+}-dependent HDAC1-3s that mainly target substrates in the nucleus (32). Indeed, we observed that exogenous expression of HDAC3, and HDAC2 to a lesser extent, but not HDAC1, was able to reduce FAAP20 acetylation induced by HA-CBP (Fig. 1, *H* and *I*). At the similar expression of HDAC1 and HDAC3, HDAC3 more efficiently deacetylated FAAP20 as well (Fig. S2, *A* and *B*). Intriguingly, a previous study has reported deacetylation of another nuclear FANC protein, FANCJ, specifically by HDAC3 (33). Together, these results indicate that FAAP20 is acetylated by p300/CBP and deacetylated primarily by HDAC3 *in vivo*.

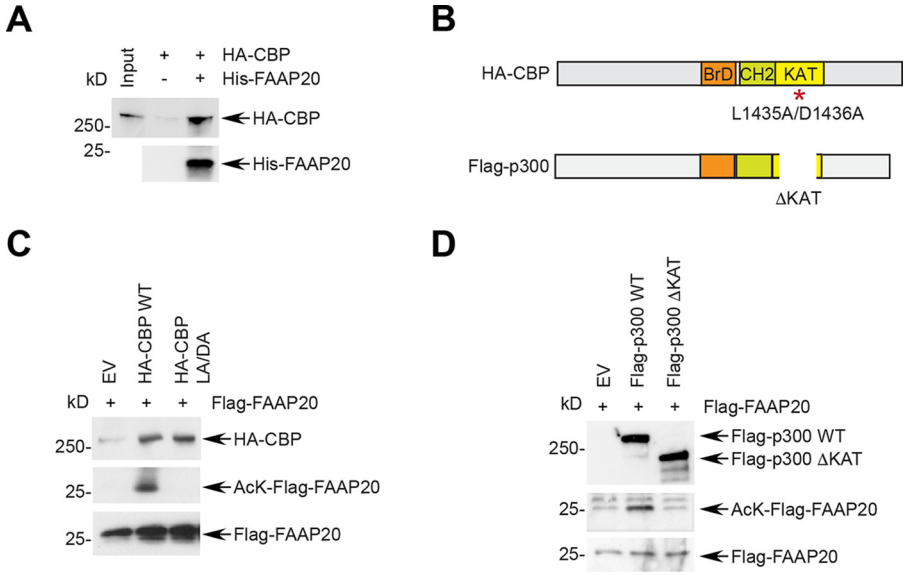

Figure 2. Catalytic activity of p300/CBP is required for FAAP20 acetylation. *A*, interaction between FAAP20 and CBP. Purified recombinant His-tagged FAAP20 was incubated with 293T cell lysates expressing HA-CBP and pulled down by Ni-NTA column, followed by Western blot analysis. *B*, schematic of the CBP and p300 proteins used in the study. Point or deletion mutations in the catalytic KAT domain are shown. *BrD,* bromo-domain; *CH2*, cysteine, histidine-rich region *2*. *C*, an intact KAT domain is required for FAAP20 acetylation. 293T cells expressing Flag-FAAP20 were transfected with HA-CBP WT or mutant (*LA/DA*: L1435A/D1436A), and cell lysates were subjected to anti-Flag IP and Western blot using an acetyl-Lys specific antibody. *D*, performed as *C*, except for transfection of Flag–p300 WT or ΔKAT mutant.

Catalytic activity of p300/CBP is required for FAAP20 acetylation

To further characterize FAAP20 acetylation, we examined its modulation by p300/CBP. Recombinant His-tagged FAAP20 pulled down HA-tagged CBP derived from cell lysates via Ni-NTA pulldown, indicating that FAAP20 directly interacts with CBP (Fig. 2*A* and Fig. S3*A*). The catalytic core of CBP and p300 contains a catalytic KAT domain responsible for lysine acetylation, which is adjacent to the bromodomain that recognizes acetylated substrates, and the CH2 region consisting of a PHD domain and a RING domain required for chromatin binding (Fig. 2*B*) (34, 35). Exogenous expression of HA-tagged CBP WT, but not the catalytically-dead mutant that has lost its interaction with acetyl-CoA, was able to induce FAAP20 acetylation (Fig. 2*C*). Similarly, the p300 mutant where the KAT domain is deleted failed to trigger FAAP20 acetylation, together indicating that the catalytic activity of p300/CBP is necessary for FAAP20 acetylation *in vivo* (Fig. 2*D*).

Lysine 152 is a major site for FAAP20 acetylation

FAAP20 is a small protein that harbors two lysine residues, Lys-83 and Lys-152, that are candidates for modification (Fig. 3*A*). These two residues are highly conserved throughout species, and it was previously shown that Lys-152 is a major site for polyubiquitination required for FAAP20 degradation (22). To determine which lysine is responsible for FAAP20 acetylation, we generated Flag-tagged FAAP20 where one or both lysine residues were mutated to disrupt its modification. Immunoblot analysis using the pan-acetylation antibody revealed that Flag-FAAP20 Lys-152 and Lys-83/Lys-152 mutants fail to be acetylated by HA-tagged CBP, whereas the Lys-83 mutation has little effect (Fig. 3, *B* and *C*). These results indicate that Lys-152 is a major site for FAAP20 acetylation, whereas Lys-83 may make minor contributions to its modification. This is consistent with the bioinformatics analysis that predicted Lys-152 as a site for FAAP20 acetylation (Fig. 1*B*). In addition, the fact that the major site for ubiquitination is also acetylated indicates that balancing the levels of ubiquitination and acetylation may modulate FAAP20 in cells.

Acetylation of FAAP20 inhibits its degradation

Protein acetylation regulates many aspects of protein property and function. To understand the role of FAAP20 acetylation, we tested several possibilities that acetylation may exert on the regulation of FAAP20. First, to examine the subcellular localization of FAAP20, we generated various GFP-tagged FAAP20 mutants. These mutants include C147A/C150A (*i.e.* disrupting the UBZ domain required for ubiquitin binding), S113A/S117A CPD (*i.e.* inhibiting FAAP20 degradation), and K83Q/K152Q acetylation-mimetic mutants (18, 22). Replacement of lysine by glutamine is a widely accepted method for mimicking lysine acetylation (36, 37). WT GFP-FAAP20 is known to primarily localize in the nucleus and exhibit distinct nuclear foci, which depends on a functional UBZ domain (18). Epifluorescence microscopy demonstrated that both CPD and KQ mutants exhibit nuclear localization with distinct foci similar to WT, indicating that acetylation does not deregulate subcellular localization of FAAP20 to the nucleus (Fig. 4*A*). Furthermore, subcellular fractionation using cytoskeleton buffer revealed that both Flag-tagged FAAP20 WT and KQ mutants show a similar pattern of localization in soluble (S) and chromatin-enriched (P) fractions, suggesting that acetylation of FAAP20 does not impact its localization (Fig. 4*B*). Because Lys-152 is within the C-terminal UBZ domain of FAAP20 that mediates its interaction with ubiquitin, we next sought to determine whether acetylation affects the ability of FAAP20 to

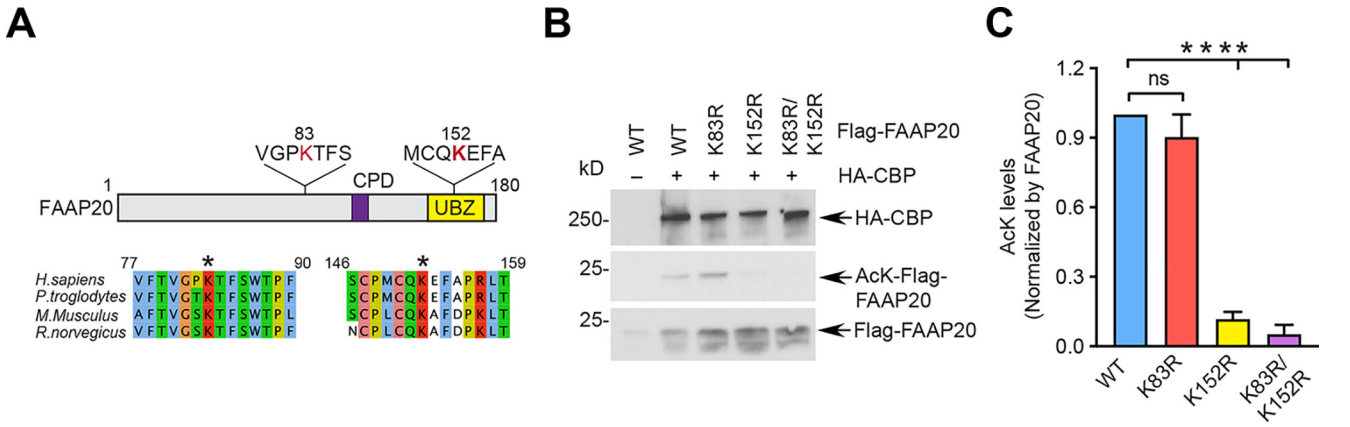

Figure 3. Lysine 152 is a major site for FAAP20 acetylation. *A*, schematic representing FAAP20 and the two potential lysine residues for acetylation. The position of lysines 83 and 152, and conservation of their flanking regions are shown. *B*, acetylation of the FAAP20 lysine mutants. 293T cells expressing Flag–AAP20 WT or various lysine mutants were transfected with HA–CBP, and cell lysates were subjected to anti-Flag IP and Western blot using an acetyl-Lys specific antibody. *C*, quantification of FAAP20 acetylation levels in *B*. *Error bar* indicates mean ± S.D., $n = 3$ from three independent experiments, ****, $p < 0.0001$; *ns*, not significant, Student's *t* test.

bind ubiquitin. Analysis of a previously published FAAP20-ubiquitin structure revealed that although Lys-152 is located within the β-sheet near the zinc-coordinating finger motif, it is projecting outward, and the ubiquitin-binding interface lies opposite to it (Fig. 4*C*) (38). A GST pulldown experiment demonstrated that GST-ubiquitin is able to pull down both the FAAP20 WT and the KQ mutant equally well, indicating that acetylation does not disrupt the ability of FAAP20 to bind to ubiquitin (Fig. 4*D*).

We then reasoned that acetylation may impact cellular FAAP20 levels as it targets the major site of ubiquitination necessary for FAAP20 degradation. When cells expressing Flag-tagged FAAP20 variants were treated with cycloheximide (CHX) to inhibit nascent protein synthesis and monitor degradation of remaining proteins, both Flag-FAAP20 KQ acetylation-mimetic and KR acetylation-deficient mutants showed increased steady-state levels and exhibited impaired degradation compared with WT, indicating that deregulation of acetylation on FAAP20 prevents its degradation (Fig. 4, *E* and *F*). Because ubiquitination and acetylation both occur on the same lysine residue, these data also suggest that acetylation may increase FAAP20 stability by protecting FAAP20 against degradation.

FAAP20 acetylation antagonizes FAAP20 ubiquitination and degradation

Because FAAP20 acetylation may be a mechanism to fine-tune the kinetics of ubiquitination that affect FAAP20 stability in cells, traditional immunoblotting of the heterologous FAAP20 protein population from bulk cell lysates may not be sensitive enough to perceive the subtle changes in FAAP20 levels. Therefore, we have established a fluorescence-based quantitative method to monitor FAAP20 stability at a single cell level, adapted from a previous proteomics study (39). In this system, N terminally Flag-tagged FAAP20 and EGFP polypeptides are independently translated from one mRNA transcript via P2A peptide-mediated ribosome skipping, such that the two proteins are expressed at a constant ratio (Fig. 5*A*). The stability of FAAP20 is analyzed by flow cytometry, where the Flag-conjugated phycoerythrin (PE) signal is represented as a mean value of the intensity, whereas EGFP fluorescence serves as an internal control to normalize the PE signal in conditions that affect FAAP20 degradation. This allows us to monitor the changes in FAAP20 stability at a single cell level. We have confirmed that transfection of Flag–FAAP20–P2A–EGFP results in independent expression of Flag–FAAP20 and EGFP, which can be monitored by PE and EGFP fluorescence, respectively (Fig. 5*B*). Transfecting increasing amounts of this bicistronic plasmid resulted in increased signals of both PE and EGFP, whereas the PE/EGFP ratio was constant, indicating that GFP fluorescence can be used as an internal control (Fig. 5*C*). Inhibition of protein degradation by the proteasome inhibitor MG132 led to an increased PE signal, whereas GFP fluorescence remained constant (Fig. 5*D*). By contrast, inhibition of protein synthesis by CHX specifically led to a decrease in the PE signal within the time we tested (Fig. 5*E*). Together, these control experiments indicate that the PE signal normalized by EGFP is a reliable readout for monitoring FAAP20 stability at the level of individual live cells.

With this system in hand, we determined the role of acetylation in FAAP20 stability in cells. Exogenous expression of CBP WT, but not the catalytic mutant, was able to increase the PE/EGFP signal, indicating that CBP activity promotes FAAP20 stabilization (Fig. 6*A*). The CBP catalytic mutant also failed to increase the endogenous levels of FAAP20 as shown by Western blot (Fig. S3*B*). In addition, both Flag–FAAP20 KQ acetylation-mimetic and KR acetylation-deficient mutants exhibited an increase in the PE/EGFP signal, confirming that the status of acetylation affects FAAP20 stability (Fig. 6*B*). Similarly, overexpression of CBP failed to further increase the PE/EGFP signal in the cells expressing the FAAP20 KQ mutant, in contrast to its ability to enhance the PE/EGFP signal of FAAP20 WT, indicating that the promotion of FAAP20 stability observed from CBP overexpression is determined by the acetylation status of FAAP20 (Fig. 6*C*). Furthermore, exogenous HDAC3 expression was able to decrease the elevated PE/EGFP signaling after CBP overexpression, suggesting that a balance between acetylation and deacetylation of FAAP20 determines FAAP20 stability

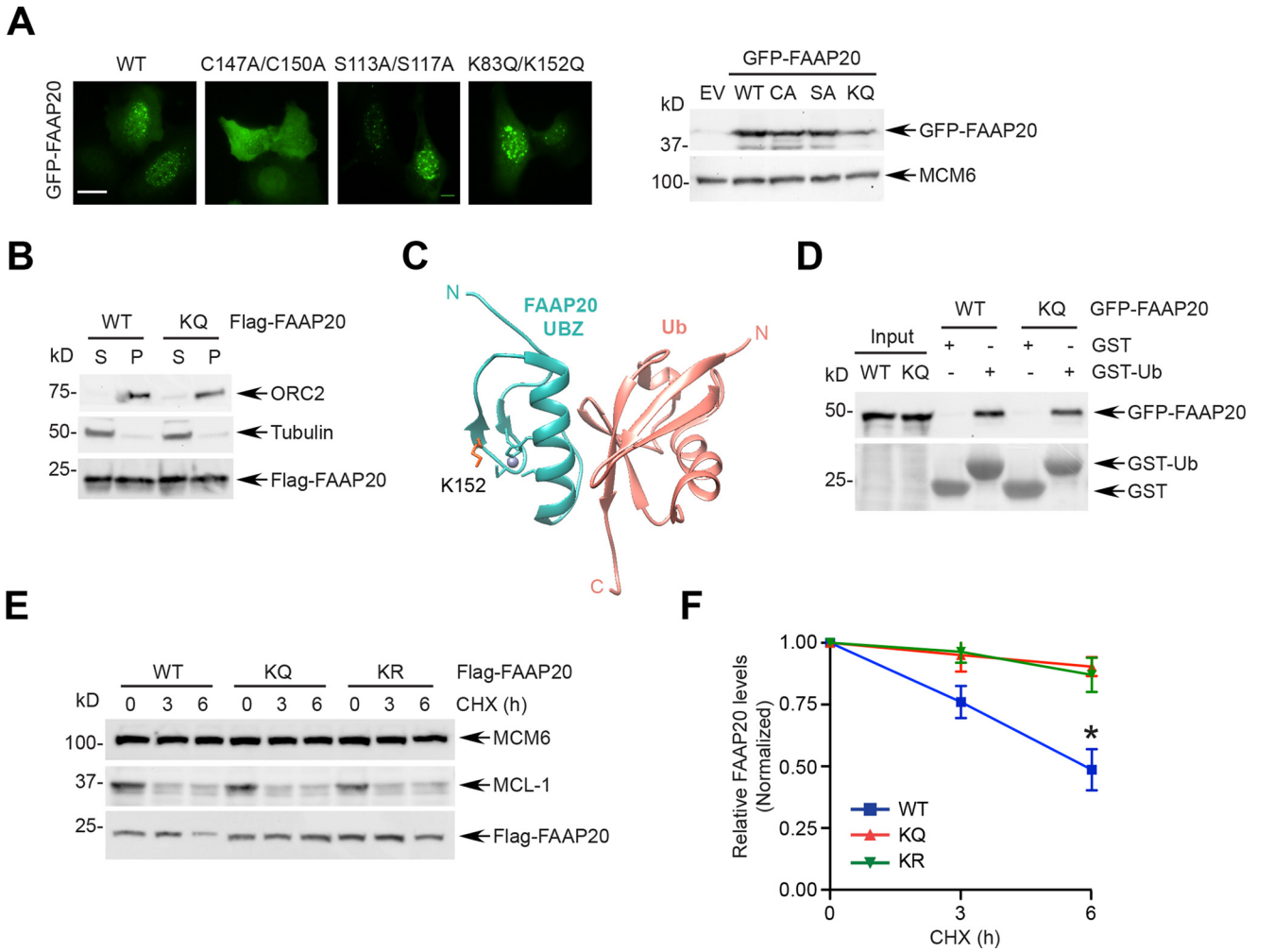

Figure 4. Acetylation of FAAP20 inhibits its degradation. *A*, *left panel*: representative images of localization of GFP-FAAP20 variants. U2OS cells were transfected with indicated GFP–FAAP20 WT or mutants, and their subcellular localization was analyzed by GFP epifluorescence. *C147A/C150A*, UBZ zinc finger mutant; *S113A/S117A*, CPD mutant; *K83Q/K152Q*, acetylation mimetic mutant. *Scale bar*: 10 μm. *Right panel*: expression of GFP-FAAP20 variants in U2OS cells. *B*, subcellular fractionation of U2OS cells transfected with Flag–FAAP20 WT or KQ (K83Q/K152Q) mutants. Tubulin and ORC2 immunoblots serve as controls for S and P fractions, respectively. *C*, a ribbon diagram of the FAAP20 UBZ–ubiquitin complex. The position of FAAP20 lysine 152 within the FAAP20 UBZ domain is shown in *red* (PDB 2MUR). *D*, interaction of the FAAP20 UBZ domain with ubiquitin *in vitro*. 293T cell lysates expressing GFP–FAAP20 WT or KQ mutants were subjected to GST pulldown using recombinant GST or GST-ubiquitin, followed by anti-GFP Western blot (*top*) or Ponceau S staining (*bottom*). *E*, degradation kinetics of Flag–FAAP20 variants. U2OS cells expressing Flag–FAAP20 WT, KQ (*K83Q/K152Q*), or KR (*K83R/K152R*) were incubated with 100 μg/ml of CHX for the indicated times, and cell lysates were analyzed by Western blot. The short-lived MCL-1 protein serves as a control for CHX treatment. *F*, quantification of Flag–FAAP20 levels in *E*. *Error bar* indicates mean ± S.D., $n = 3$ from three independent experiments, *, $p < 0.05$, KQ or KR compared with WT, Student's *t* test.

(Fig. 6*D*). Finally, an *in vivo* ubiquitination assay using Ni-NTA pulldown revealed that polyubiquitination of FAAP20 is markedly reduced by CBP overexpression, further confirming that acetylation of FAAP20 competes with ubiquitination to antagonize FAAP20 degradation (Fig. 6*E*). Taken together, these results support the notion that FAAP20 acetylation antagonizes FAAP20 ubiquitination and degradation.

Deregulation of FAAP20 acetylation disrupts FANCD2 activation

Destabilization of FAAP20 impairs the integrity of the FA core complex, leading to a defect in the activation of the FA pathway. Therefore, we next wanted to determine whether down-regulating FAAP20 acetylation disrupts the balance of FAAP20 levels, leading to the destabilization of FAAP20 and impaired FANCD2 monoubiquitination in response to DNA damage. Knockdown of either p300 or CBP in U2OS cells caused a significant decrease in damage-induced FANCD2 monoubiquitination from mitomycin C (MMC), an ICL-inducing clastogen (Fig. 7*A*). Induction of CHK1 phosphorylation at serine 345 was similar across the knocked down samples, indicating that DNA damage signaling is not affected by p300 or CBP depletion. It is plausible that the observed effect results from a pleotropic consequence of disrupting global acetylation in cells. However, exogenous expression of the Flag–FAAP20 KQ acetylation-mimetic mutant in p300- or CBP-depleted cells was able to restore FANCD2 monoubiquitin levels after MMC-induced DNA damage, indicating that defects in FANCD2 activation in p300/CBP-depleted cells are at least in part caused by a defect in the FA core complex due to the loss of FAAP20 and can be rescued by the FAAP20 protein that is refractory to degradation (Fig. 7*A*). Furthermore, cell cycle analysis using 5-ethynyl-2'-deoxyuridine (EdU) uptake did not reveal any major

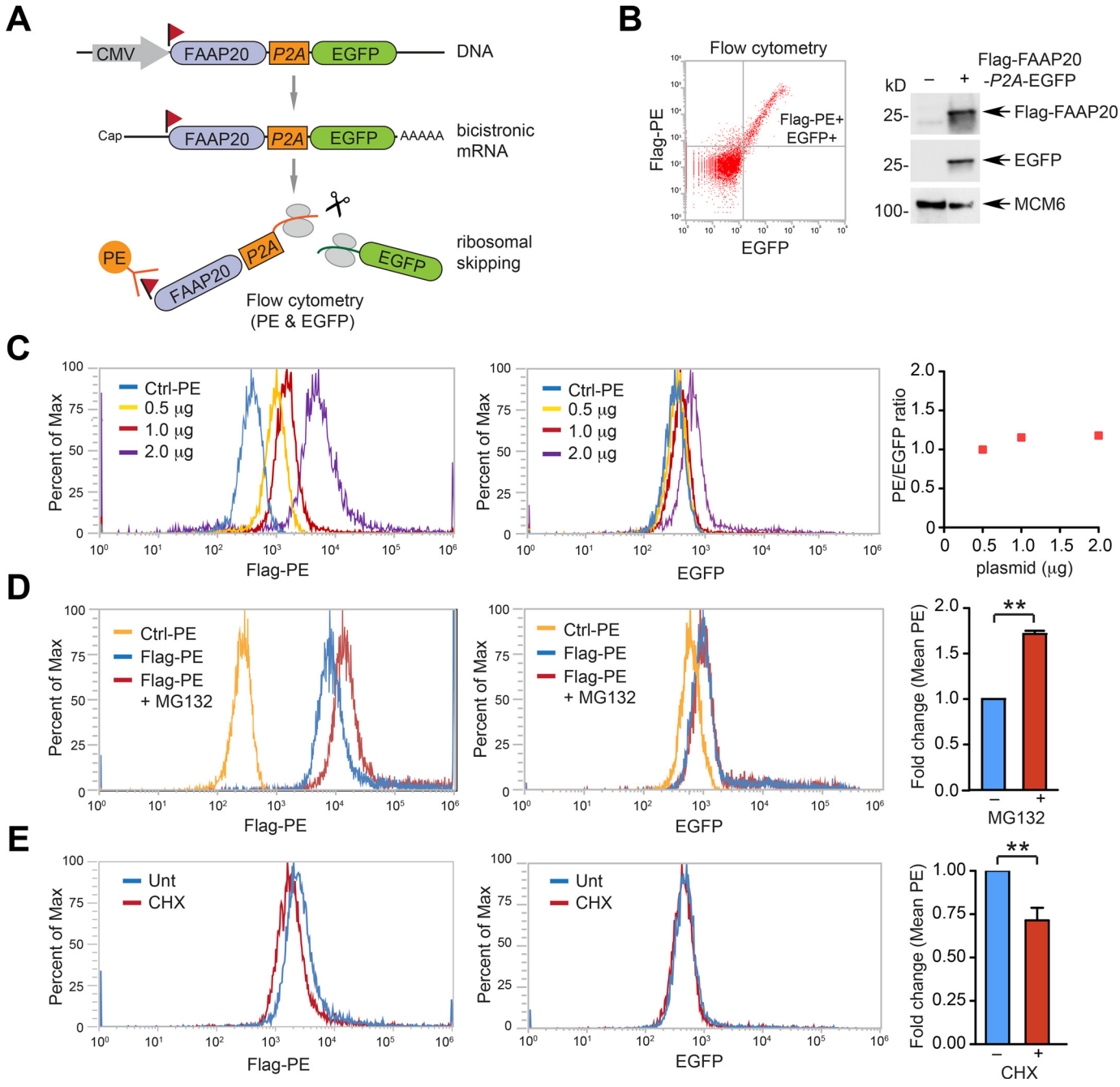

Figure 5. A fluorescence-based system to monitor FAAP20 stability. *A*, schematic of the FAAP20–P2A–EGFP reporter construct. A CMV promoter drives the transcription of the single mRNA transcript for both Flag–FAAP20 and EGFP. Ribosomal skipping of glycyl-prolyl peptide bond formation in a P2A "self-cleaving" peptide leads to the generation of Flag–FAAP20 and EGFP polypeptides at an equal molar ratio. EGFP serves as an internal control for transfection, whereas Flag–FAAP20 is stained by a PE-conjugated anti-Flag antibody for fluorescence quantification. *B*, *left panel*: a representative FACS plot showing Flag–PE$^+$/EGFP$^+$ cells in the *upper right quadrant*. *Right panel*: immunoblots confirming the production of Flag–FAAP20 and EGFP in U2OS cells transfected with Flag–FAAP20–P2A–EGFP. *C*, *left panel*: FACS histogram of Flag–PE and EGFP from U2OS cells transfected with the indicated amount of the Flag–FAAP20–P2A–EGFP reporter construct. *Ctrl-PE* indicates cells stained with a PE-conjugated IgG2a control antibody. *Right panel*: mean PE/EGFP values from the various amounts of plasmid transfection are plotted. *D*, *left panel*: U2OS cells expressing the reporter construct were treated with 10 μM MG132 for 6 h and analyzed by FACS. *Right panel*: fold-change of the Flag–PE mean value normalized by EGFP. *Error bar* indicates mean ± S.D., $n = 2$ from two independent experiments, **, $p < 0.01$, Student's *t* test. *E*, *left panel*: U2OS cells expressing the reporter construct were treated with 100 μg/ml of CHX for 5 h and analyzed by FACS. *Right panel*: fold-change of the Flag–PE mean value normalized by EGFP. *Error bar* indicates mean ± S.D., $n = 3$ from three independent experiments, **, $p < 0.01$, Student's *t* test.

disruption of the cell cycle upon p300 or CBP knockdown within the time we tested, suggesting that an aberrant cell cycle is not sufficient to account for the defect in FANCD2 monoubiquitination noted above (Fig. 7*B*). In contrast, we observed that co-depletion of p300 and CBP markedly reduced cells in the S phase with a concomitant increase of cells in G1, indicating that depletion of p300 and CBP together causes a defect in the G1/S transition (Fig. 7*B*). Indeed, co-knockdown of p300 and CBP abrogated damage-induced FANCD2 monoubiquitination, which could not be rescued by Flag-FAAP20 KQ

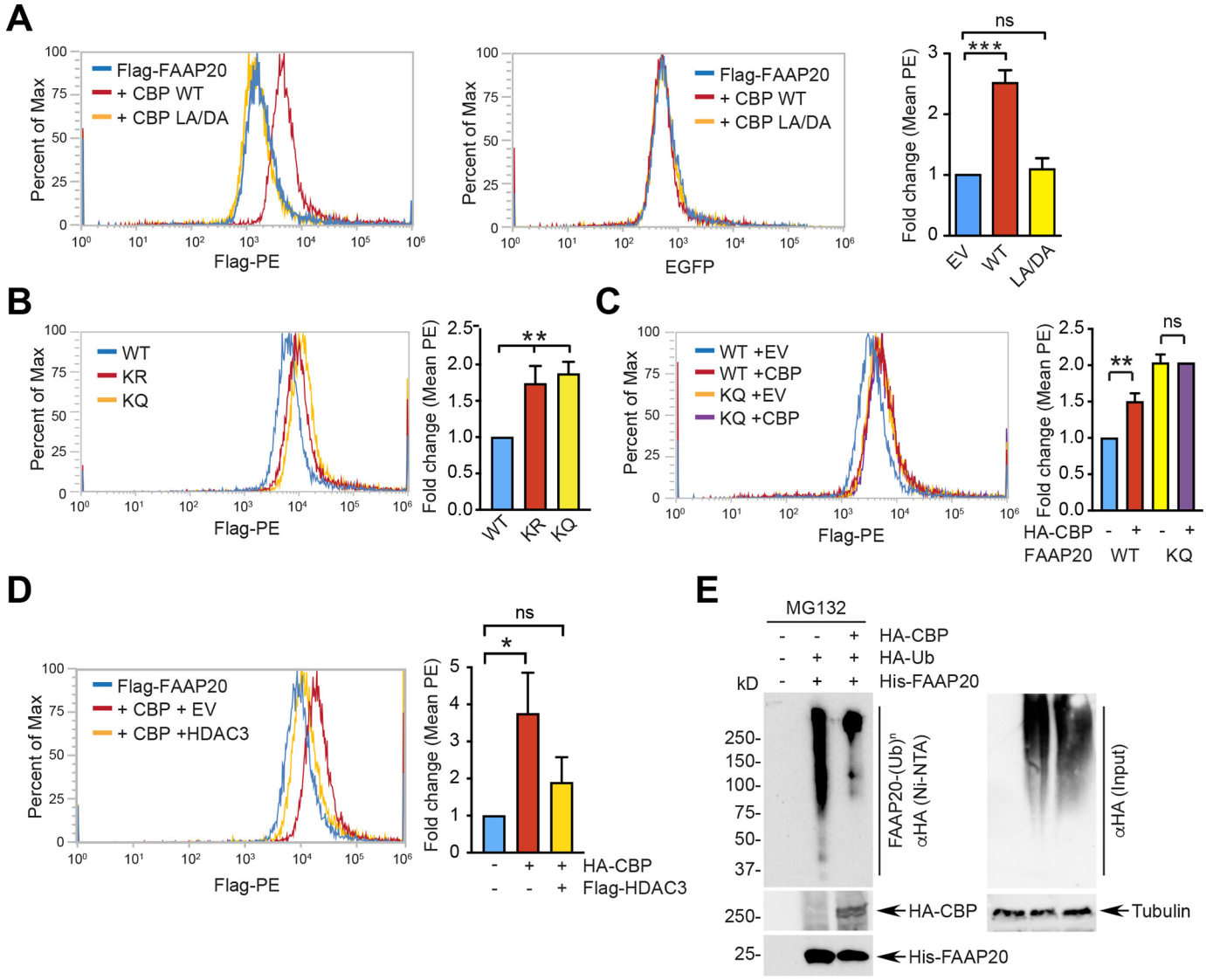

Figure 6. FAAP20 acetylation antagonizes FAAP20 ubiquitination and degradation. *A, left panel*: FACS histogram of Flag–PE and EGFP from the reporter-expressing U2OS cells transfected with HA–CBP WT or L1435A/D1436A mutant (EV). *Right panel*: fold-change of the Flag–PE mean value normalized by EGFP. *Error bar* indicates mean ± S.D., $n = 3$ from three independent experiments, ***, $p < 0.001$, *ns*, not significant, Student's *t* test. *B, left panel*: FACS histogram of Flag–PE from U2OS cells transfected with Flag–FAAP20–P2A–EGFP WT, K83R/K152R, or K83Q/K152Q. *Right panel*: fold-change of the Flag–PE mean value normalized by EGFP. *Error bar* indicates mean ± S.D., $n = 3$ from three independent experiments, **, $p < 0.01$, Student's *t* test. *C, left panel*: FACS histogram of Flag–PE from the reporter-expressing U2OS cells (WT or KQ) transfected with HA–CBP (*versus* EV). *Right panel*: fold-change of the Flag–PE mean value normalized by EGFP. *Error bar* indicates mean ± S.D., $n = 3$ from three independent experiments, **, $p < 0.01$, *ns*, not significant, Student's *t* test. *D, left panel*: FACS histogram of Flag–PE from the reporter-expressing U2OS cells transfected with HA–CBP alone or together with Flag–HDAC3 (*versus* EV). *Right panel*: fold-change of the Flag–PE mean value normalized by EGFP. *Error bar* indicates mean ± S.D., $n = 3$ from three independent experiments, *, $p < 0.05$, *ns*, not significant, Student's *t* test. *E*, Ni-NTA pulldown of polyubiquitinated His–FAAP20. 293T cells were transfected with the indicated plasmids, treated with 10 μM MG132 for 4 h, and subjected to Ni-NTA pulldown under denaturing conditions to enrich His–FAAP20 polyubiquitination by HA-ubiquitin.

overexpression, indicating that G1/S cell cycle arrest is predominantly responsible for the defect in FANCD2 activation in this condition (Fig. 7*C*). Nevertheless, knocking down both p300 and CBP accelerated the degradation of endogenous FAAP20 when its synthesis was inhibited by cycloheximide, indicating that FAAP20 becomes unstable when p300 and CBP are not present in cells (Fig. 7*D*). This further confirms that FAAP20 is a valid determinant for the activation of FANCD2 in p300- or CBP-depleted cells. Moreover, we observed that overexpression of HDAC2 and HDAC3 is able to down-regulate FANCD2 monoubiquitination, which can be antagonized by exogenous expression of Flag–FAAP20 KQ (Fig. 7*E*). Taken together, these results demonstrate that down-regulation of FAAP20 acetylation, either by depletion of p300/CBP or overexpression of HDACs, causes a defect in FANCD2 monoubiquitination upon DNA damage in a FAAP20-dependent manner, indicating that disruption of FAAP20 acetylation renders FAAP20 unstable, compromising the integrity of the FA core complex necessary for FANCD2 activation.

To further understand the physiological role of FAAP20 acetylation in modulating the FA pathway, we examined the acetylation of FAAP20 in response to DNA damage and its contribution to DNA repair. We previously showed that controlled degradation of FAAP20, prompted by its phosphorylation at

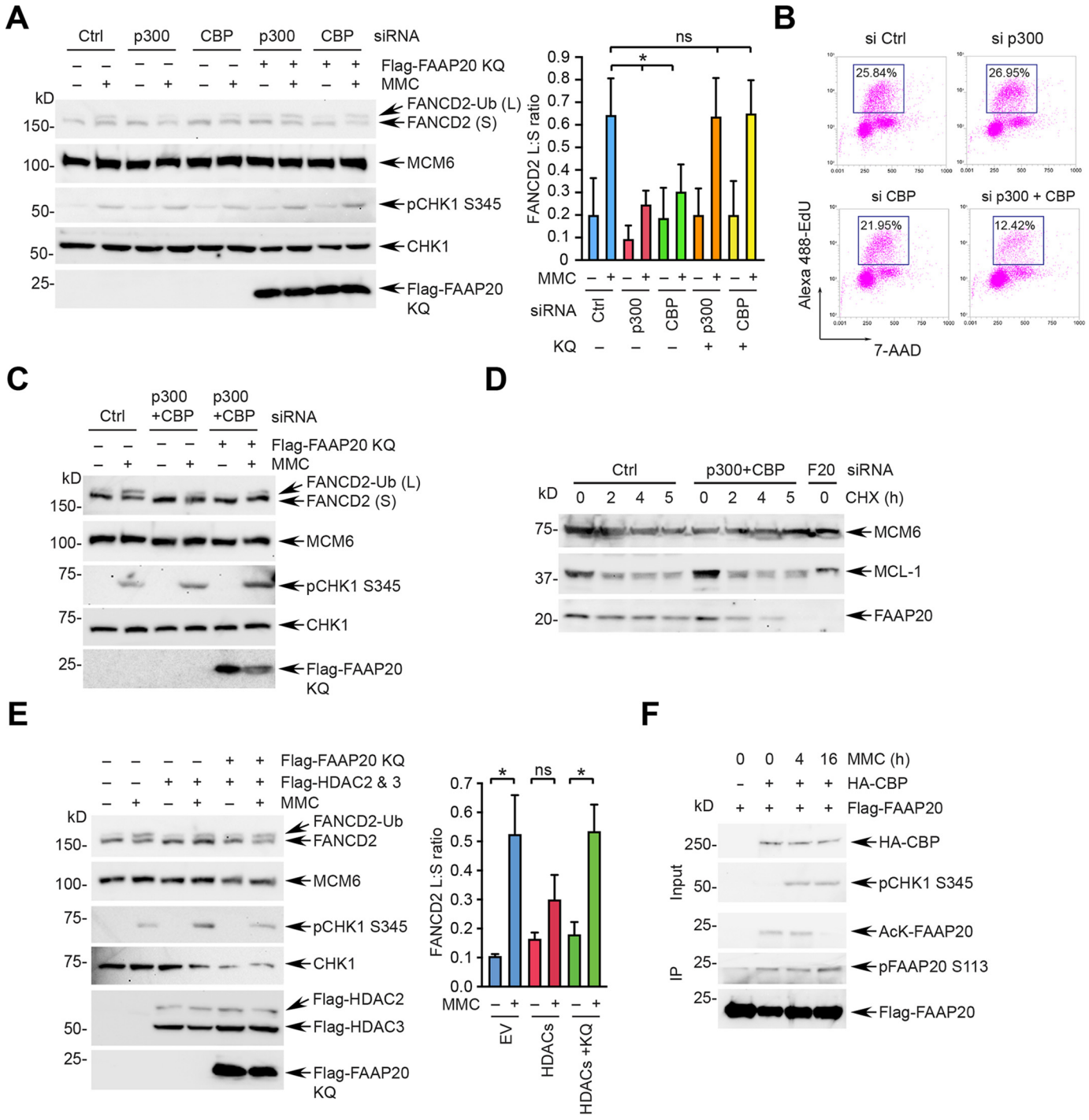

Figure 7. Deregulation of FAAP20 acetylation impairs FANCD2 activation. *A*, *left panel*: defective FANCD2 activation upon depletion of p300 or CBP. U2OS cells transfected with the indicated siRNA were treated with 100 ng/ml of MMC for 6 h, and cell lysates were analyzed by Western blot. Where indicated, cells were transfected with pcDNA3–Flag–FAAP20 K83Q/K152Q (*versus* empty vector) for 40 h before MMC treatment. *Right panel*: quantification of the FANCD2–Ub:FANCD2 ratios (*L*:*S*), via Fiji (ImageJ). *Error bar* indicates mean ± S.D., $n = 3$ from three independent experiments, *, $p < 0.05$, *ns*, not significant, Student's *t* test. *B*, representative FACS plots of EdU cell cycle analysis. EdU^+ S phase cells are gated, and % cell populations are represented as an average from two independent experiments. *C*, the FAAP20 KQ cannot rescue the FANCD2 activation defect caused by co-depletion of p300 and CBP. U2OS cells transfected with the indicated siRNA were treated with 100 ng/ml of MMC for 6 h, and cell lysates were analyzed by Western blot. Where indicated, cells were transfected with pcDNA3–Flag–FAAP20 KQ (*versus* empty vector) for 40 h before MMC treatment. *D*, depletion of p300 and CBP accelerates the degradation of endogenous FAAP20. U2OS cells transfected with siRNA control or p300 and CBP together were treated with 100 μg/ml of CHX for the indicated times, and endogenous FAAP20 levels were analyzed by Western blot. siRNA FAAP20-transfected cells were used for control to confirm the specificity of FAAP20 signals. *E*, *left panel*: defective FANCD2 activation upon overexpression of HDACs. U2OS cells were co-expressed with Flag–HDAC2 and HDAC3 along with an empty vector or Flag–FAAP20 KQ, and cell lysates were analyzed by Western blot. *Right panel*: quantification of the FANCD2–Ub:FANCD2 ratios (*L*:*S*), via Fiji (ImageJ). *Error bar* indicates mean ± S.D., $n = 2$ from two independent experiments, *, $p < 0.05$, *ns*, not significant, Student's *t* test. *F*, U2OS cells transfected with the indicated plasmids were treated with 1 μM MMC for the indicated times, and chromatin-enriched fractions were subjected to anti-Flag IP, followed by Western blot using acetyl-Lys specific and FAAP20 pS113 CPD antibodies.

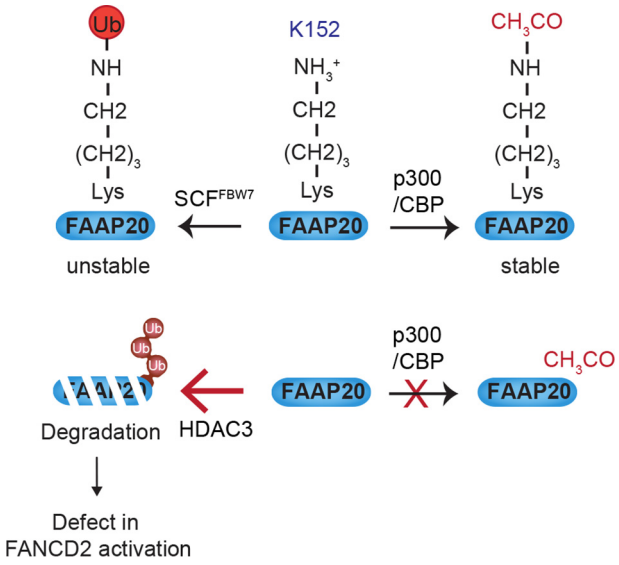

Figure 8. A model depicting the regulation of FAAP20 stability by acetylation signaling. *Top panel*: cellular FAAP20 levels were determined by the competitive modification of Lys-152, which undergoes either ubiquitination by the SCF^{FBW7} ubiquitin E3 ligase to promote degradation, or acetylation by the p300/CBP acetyltransferase to antagonize degradation. *Bottom panel*: disruption of FAAP20 acetylation either by the depletion of p300/CBP or by the overexpression of HDAC3 renders the lysine residue of FAAP20 susceptible to polyubiquitination, leading to FAAP20 degradation and defective FANCD2 activation.

CPD under DNA damage, is necessary for the completion of DNA ICL repair in a timely fashion by inactivating the FA core complex (22). Intriguingly, whereas we did not observe any significant induction of FAAP20 acetylation upon MMC treatment, we noticed that FAAP20 acetylation is down-regulated upon prolonged incubation of MMC (Fig. 7*F*). This coincided with increased phosphorylation at the degron motif that triggers FAAP20 degradation by SCF^{FBW7}, indicating that down-regulation of FAAP20 acetylation during DNA repair may prime FAAP20 ubiquitination for its controlled turnover. Thus, the cellular DNA damage response signaling that regulates FAAP20 acetylation may fine-tune the FAAP20 degradation process to balance FAAP20 levels in the FA core complex, contributing to the completion of DNA repair.

Discussion

Acetylation as a new mechanism for FAAP20 regulation

In this study, we present evidence that acetylation of FAAP20 plays a regulatory role in governing FAAP20 degradation. We propose that the acetylation of Lys-152 in FAAP20 prevents the ubiquitination of the common lysine residue, thereby preventing proteasome-dependent degradation of FAAP20 mediated by the SCF^{FBW7} ubiquitin E3 ligase. We have demonstrated that the p300/CBP KATs are responsible for the acetylation of FAAP20, primarily at Lys-152, whereas one or more of the class I deacetylases, predominantly HDAC3, antagonizes its modification. Hence, cellular levels of FAAP20 are determined by the balanced action between acetylation signaling and ubiquitin-dependent proteasomal degradation (Fig. 8). Accordingly, decreased acetylation by down-regulation of p300/CBP activity or enhanced HDAC3 activity sensitizes FAAP20 to ubiquitination and subsequent degradation, thereby resulting in compromised FA core complex activity and defective FANCD2 activation. Under the DNA damage signaling, down-regulation in FAAP20 acetylation levels may also prime regulated FAAP20 degradation that contributes to the inactivation of the FA core complex and timely completion of DNA ICL repair. Together, our study elucidates a new competition mechanism between ubiquitination and acetylation that works on a common lysine residue to control the stability of FAAP20. Of note, a previous study has demonstrated a similar competition mechanism between acetylation and ubiquitination that controls protein stability, in which the cellular levels of Smad7 in transforming growth factor β signaling is regulated by the acetylation of the lysine residues targeted by ubiquitin E3 ligase Smurf1-mediated ubiquitination (40). Thus, modulation of protein ubiquitination or acetylation on the same residue may be a general mechanism that cells have devised to fine-tune protein stability in various cellular processes.

Proteolysis of FAAP20 constitutes a key mechanism to regulate the function of the FA core complex. By directly interacting with the FANCA subunit and masking its SUMO-targeted degron, FAAP20 prevents proteasomal degradation of FANCA and maintains the integrity of the FA core complex (18, 21). As a result, deficiency of FANCA or FAAP20 results in defective damage-induced FANCD2 monoubiquitination. Accordingly, the *FANCA* loss-of-function mutations are most prevalent among FA patients (41). Interestingly, several somatic mutations derived from cancer patients are known to disrupt the FAAP20–FANCA interaction, suggesting that keeping the FAAP20–FANCA interaction to preserve FA core complex integrity may be crucial for suppressing genome instability and limiting tumorigenesis (21). As a small protein, FAAP20 is subjected to rapid degradation that may act as a switch to regulate the dynamics of the FA core complex both in an unstressed condition and under DNA damage. Integrated phosphorylation-ubiquitin signaling is known to control FAAP20 degradation. We have previously shown that glycogen synthase kinase β-dependent phosphorylation of the CPD motif provides a docking site for recruiting the SCF^{FBW7} ubiquitin E3 ligase complex to polyubiquitinate Lys-152 and degrade FAAP20, indicating that the phosphorylation status of CPD determines the kinetics of FAAP20 degradation (22). Importantly, a structural change mediated by the PIN prolyl isomerase that isomerizes the phosphorylated Ser^{48}–Pro^{49} motif, located in the N terminus of FAAP20, promotes its interaction with the PP2A phosphatase, thereby down-regulating CPD phosphorylation and antagonizing FAAP20 degradation (23). Here, we have unveiled Lys-152 as a primary acceptor residue for acetylation, which competes with ubiquitination to block FAAP20 degradation. Thus, multiple independent posttranslational modifications, including phosphorylation, ubiquitination, SUMOylation, and acetylation, cooperate to control proteasomal degradation of FAAP20 and FANCA in the FA core complex, through which FANCD2 activation is modulated. Understanding the physiological cellular signaling that coordinates these modifications to govern FANCA and FAAP20 levels during cell cycle progression and upon DNA damage would be an important future direction to pursue.

Posttranslational modifications in the FA core complex

Our results highlight another layer in the complex posttranslational regulatory mechanisms that control FA core complex activity and function. It is still unclear why the FA core complex exists as a multisubunit complex that is composed of at least 10 proteins without any obvious homology or evolutionary relationship. Although the FANCL subunit alone exhibits catalytic activity mediated by a RING domain, mutation of individual *FANC* genes is sufficient for abrogating the E3 ligase function of the FA core complex in cells, indicating that the other subunits work as structural and regulatory elements to support the functional integrity of the FA core complex. A modular feature of the FA core complex revealed by a series of *in vitro* biochemical experiments suggests that individual subunits play distinct roles required for achieving optimal activity of the FA core complex (12, 13). Intriguingly, a recently published structure revealed that the FA complex dimerizes asymmetrically, wherein two FANCL subunits form into distinct conformations and arrange in an asymmetric manner within the B-L-100 catalytic module, suggesting that individual FANCL has a different role in positioning the ID complex and promoting the monoubiquitination of FANCD2 (16). In addition, a wide range of posttranslational modifications in the individual subunits of the FA core complex implicates them in fine-tuning the signaling of the FA pathway during DNA replication and in response to DNA damage. For instance, ATR-dependent phosphorylation is known to activate multiple components of the FA pathway. Inhibition of FANCM phosphorylation at Ser-1045 disrupts CHK1 phosphorylation and FANCD2 monoubiquitination from DNA replication stress (42). FANCE phosphorylation at Thr-346 and Ser-374 and FANCA phosphorylation at Ser-1449 by the ATR-CHK1 checkpoint are known to promote the function of the FA core complex (43, 44). FANCD2 phosphorylation at Thr-691 and Ser-717 as well as phosphorylation of a cluster of SQ/TQ sites on FANCI potentiates FANCD2 monoubiquitination (45, 46). Furthermore, different levels of ATR-mediated FANCI phosphorylation are known to switch the function of FANCI either to dormant origin firing or to DNA repair, depending on the severity of the DNA replication stress (47). Conversely, FANCM hyperphosphorylation on a β-TRCP phosphodegron and subsequent FANCM degradation inactivates the FA core complex during mitosis (48). Similarly, SUMOylation of FANCD2 promotes the extraction and degradation of chromatin-bound FANCD2 at DNA lesions to down-regulate FANCD2 activity, indicating that multiple posttranslational modifications fine-tune FA pathway signaling (49).

Regulation of DNA repair by acetylation

Protein acetylation modulates a variety of cellular processes, and as revealed in this study, the genome maintenance pathway is no exception. Originally identified as a modifier of histones that regulates transcription and chromatin remodeling, the p300/CBP KATs are also known for regulating the recruitment of DNA repair factors to DNA lesions to facilitate repair (30). p300/CBP is generally thought of as a tumor suppressor, and the *EP300* and *CREBBP* genes (encoding p300 and CBP, respectively) are mutated in several solid tumors and hematological malignancies (50, 51). Mutations in these genes are also responsible for some causes of Rubinstein-Taybi syndrome, which is often a predisposition to brain tumors and leukemia (52). Emerging evidence indicates that p300/CBP contributes to genome stability by acetylating specific DNA replication and repair factors to regulate their function in the DNA damage response (DDR), through a variety of distinct mechanisms. Several examples include: FANCJ acetylation that determines DNA repair choice within the FA pathway (33); PARP1 acetylation that blocks histone ADP-ribosylation and shut downs PARP activity (53); PCNA acetylation that promotes PCNA unloading and degradation during nucleotide excision repair (54); DNA2 helicase/nuclease acetylation that increases its affinity to DNA (55); RECQL4 helicase acetylation that regulates subcellular localization (56); and KU70 acetylation that affects protein–protein interactions and DNA binding (57, 58). Intriguingly, several studies indicate that p300/CBP activity is upregulated in response to DNA damage, indicating that p300/CBP may undergo posttranslational modifications from DDR signaling (54, 59, 60). Indeed, p300 is known to be phosphorylated at Ser-106 by ATM following γ-irradiation to enhance its activity, but other unknown modifications may also be involved in response to different genotoxic stresses (61). In addition, the interaction between p300/CBP and ATR increases under DNA replication stress, which promotes CHK1 phosphorylation, indicating that p300/CBP may exert a broader role on checkpoint activation and recruitment of DNA repair factors to sites of DNA damage along with modulation of the chromatin structure (62). It is unknown if ICL-induced stalling of DNA replication forks triggers DDR signals that change the activity of p300/CBP. Thus, it would be important to investigate if this may influence the dynamics of the FA pathway during DNA ICL repair. Collectively, our discovery of FAAP20 acetylation reinforces the idea that lysine acetylation is a key mechanism through which DNA repair is regulated and genome integrity is maintained. Building on this idea would provide insights into how the deregulation of acetylation signaling, such as HDAC inhibition used in the clinic, affects tumor cell survival and sensitivity to chemotherapeutics. This knowledge may lead to the development of new therapeutic strategies to exploit DNA repair regulation by modulating the acetylation of key genome maintenance proteins.

Experimental procedures

Cell culture and plasmid construction

U2OS and 293T cell lines were acquired from the American Tissue Culture Collection (ATCC). Cells were cultured in Dulbecco's modified Eagle's medium at 37 °C, 5% CO_2 supplemented with 10% fetal bovine serum and 1% penicillin/streptomycin, following standard culture conditions and procedures. pcDNA3.1–Flag–FAAP20 and EGFP–FAAP20 were previously described (18). Point mutations were introduced using the QuikChange II XL site-directed mutagenesis kit (Agilent Technologies) and confirmed by DNA sequencing. To construct pcDNA3.1–Flag–FAAP20–P2A–EGFP, FAAP20 cDNA (clone ID: OHu13709, GenScript) was first ligated to pcDNA3.1–P2A–EGFP via 5' BamHI and 3' EcoRI restriction sites, and an

N-terminal Flag tag was inserted in front of cDNA using GenEZ ORF cDNA clones and mutagenesis service (GenScript). The same FAAP20 cDNA was cloned into the pcDNA3-N–His_6 vector (GenScript) via 5' BamHI and 3' EcoRI restriction sites to generate an N-terminal His-tagged FAAP20-expressing plasmid. Expression plasmids for HA–CBP, HA–p300, Flag–TIP60, Flag–MOF, Flag–PCAF, Flag–p300, Flag–p300 ΔHAT, Flag–HDAC1, and Flag–HDAC2 were a kind gift from Dr. Sharon Cantor (University of Massachusetts, Worcester, MA). pcDNA3–HDAC3–Flag was a gift from Dr. Eric Verdin (Addgene plasmid No. 13819). pcDNA3β–Flag–CBP–HA and pcDNA3β–Flag–CBP–HA L1435A/D1436A were a gift from Dr. Tso-Pang Yao (Addgene plasmid numbers 32908 and 32906).

Plasmids and siRNA transfection

Plasmid transfection was performed using GeneJuice (Millipore) in Opti-MEM (Thermo Fisher) according to the manufacturer's protocols. The ratio of DNA/Genejuice was 1 μg/2 μl. siRNA duplexes were transfected at 25 nM using Lipofectamine RNAiMAX (Thermo Fisher). siRNA oligonucleotides were synthesized by Qiagen. The following siRNA target sequences were used; control, 5′-GGGTATCGACGATTACAAA-3′; p300, 5′-GGGAATGAATGTAACAAAT-3′; CBP, 5′-GATGCTGCTTCCAAACATA-3′.

Antibodies and chemicals

The following antibodies were used for Western blotting: FAAP20 (HPA038829, Sigma-Aldrich), pFAAP20 S113 (in-house) (22), acetylated-lysine (No. 9441, Cell Signaling Technology), pCHK1 S345 (No. 2341, Cell Signaling Technology), Flag (M2, F1804, Sigma-Aldrich), Flag (M2, F3165, Sigma-Aldrich), GFP (B-2, sc-9996, Santa Cruz), HA (2-2.2.14, No. 26183, Thermo Fisher), MCM6 (H-8, sc-393618, Santa Cruz), Tubulin (B-7, sc-5286, Santa Cruz), PCNA (PC-10, sc-56, Santa Cruz), and MCL-1 (16225-1-AP, Proteintech). Mitomycin C (M5350), Z-Leu-Leu-Leu-al (MG132; C2211), cycloheximide (C4859), and trichostatin A (T1592) were purchased from Sigma-Aldrich. Drugs were used at the concentrations indicated in the figure legends.

Western blotting, immunoprecipitation, fractionation

Cells were lysed in NETN300 buffer (1% Nonidet P-40, 300 mM NaCl, 0.1 mM EDTA, and 50 mM Tris (pH 7.5)) supplemented with protease inhibitor mixture (Roche) and 10 μM TSA (T1952, Sigma-Aldrich). Lysates were resolved by SDS-PAGE, transferred onto PVDF membranes (Millipore), and antibodies were detected by an enhanced chemiluminescence method (Pierce ECL, or SuperSignal West Pico Plus, Thermo Fisher) using either Hyblot Cl autoradiography film (Denville Scientific) or iBright CL1000 Western blotting imaging systems (Thermo Fisher). To detect the acetylation of immunoprecipitated FAAP20 induced by HA-CBP, 293T cells were lysed in NETN150 buffer (1% Nonidet P-40, 150 mM NaCl, 0.1 mM EDTA, and 50 mM Tris (pH 7.5)), supplemented with protease inhibitor mixture (Roche) and 10 μM TSA, and centrifuged at 15,000 rpm at 4 °C. 5% of the input was saved, and cell lysates were incubated with anti-Flag M2 affinity gel (A2220, Sigma-Aldrich) with gentle rocking at 4 °C for 3 h. Agarose resins were washed three times with NETN150 buffer, and immune complexes were released by boiling in 2× Laemmli sample buffer. To detect endogenous FAAP20 acetylation, 293T cells were transfected with siRNA and treated with 400 nM TSA for 16 h. Cells were lysed in NETN150 buffer, supplemented with protease inhibitor and 10 μM TSA, and cell lysates were incubated with anti-FAAP20 antibody (Sigma-Aldrich) at 4 °C for 4 h and with protein G-Sepharose 4 fast flow (GE Healthcare) for an additional 2 h. Resins were washed three times with NETN150 buffer, and immune complexes were eluted with 0.1 M glycine (pH 2.5) at room temperature for 10 min twice. Protein samples were neutralized by 1 M Tris-HCl (pH 8.0), precipitated with TCA by adding 1 volume of 100% TCA to 4 volumes of protein samples on ice for 20 min, and centrifuged at 15,000 rpm at 4 °C. Precipitated protein pellets were resuspended with 1 M Tris-HCl (pH 8.0) and boiled with 2× Laemmli sample buffer for SDS-PAGE. Subcellular fractionation was performed as previously described (22). Briefly, cells were lysed using cytoskeleton buffer (10 mM Tris (pH 6.8), 100 mM NaCl, 300 mM sucrose, 3 mM $MgCl_2$, 1 mM EGTA, 1 mM EDTA, and 0.1% Triton X-100) for 5 min on ice. After centrifugation at 1,500 × *g* for 5 min, the supernatant (S) was separated from the pellet (P), and pellets were sequentially lysed in PBS and 2× boiling lysis buffer (50 mM Tris-Cl (pH 6.8), 2% SDS, and 850 mM β-mercaptoethanol).

Fluorescence microscopy

To conduct GFP epifluorescence, cells were transfected and grown on coverslips, fixed with 4% paraformaldehyde for 10 min at room temperature, then washed three times with PBS, and mounted with 4′,6-diamidino-2-phenylindole-containing mounting medium (Vector Laboratory). Images were captured using the Eclipse Ts2R-FL inverted fluorescence microscope (Nikon) equipped with the Nikon DSQi2 digital camera, and analyzed via NIS-Elements software (Nikon).

Flow cytometry-based protein stability profiling

U2OS cells were harvested and fixed with the eBioscience Foxp3/transcription factor fixative solution (Thermo Fisher) for 15 min. Cells were diluted with PBS, 1% BSA and spun down at 4,000 rpm for 5 min. Pellets were permeabilized with PBS, 0.3% Triton X-100 for 5 min and washed once with the Foxp3/transcription factor staining buffer (Thermo Fisher). Subsequently, cells were incubated with PE-conjugated rat anti-Flag antibody (1:25, No. 637309, Biolegend) for 1 h. PE-conjugated rat IgG2a, κ isotype antibody was used as a control, and an unstained control was incubated with staining buffer only. Cells were washed with staining buffer once, resuspended in 500 μl of staining buffer, and analyzed by the Attune NxT acoustic focusing flow cytometer (Thermo Fisher). Fluorophores were excited with a 400-nm blue laser, and PE and GFP fluorescence were detected with BL2 (574/26) and BL1 (530/30) emission filters, respectively. Mean PE intensity was determined by the integrated Attune NxT software version 2.7 (Thermo Fisher) and normalized by the mean intensity of GFP.

GST pulldown assay

GST pulldown was performed as previously described. For the interaction between GST-Ub and GFP-FAAP20, GST or GST-Ub was expressed using the *Escherichia coli* BL21 (DE3) expression strain induced with 0.5 mM isopropyl β-D-1-thiogalactopyranoside (Sigma-Aldrich) at 37 °C for 4 h. Cells were lysed in PBS with lysozyme, sonicated, and further incubated with 1% Triton X-100. Cell lysates were recovered by centrifugation at 15,000 rpm at 4 °C for 15 min and incubated with GSH-Sepharose beads (GE Healthcare). After washing, the beads were incubated with lysates from 293T cells expressing GFP–FAAP20 in NETN150 buffer at 4 °C for 3 h followed by three washes with NETN150. The beads were resuspended with 2× Laemmli sample buffer, boiled, and protein complexes were analyzed by SDS-PAGE.

In vivo ubiquitin assay

In vivo ubiquitin assays were performed under denaturing conditions. MG132-treated cells were harvested, resuspended with Buffer A (6 M guanidine-HCl, 0.1 M $Na_2HPO_4/NaH_2PO_4{\cdot}H_2O$, 10 mM imidazole, pH 8.0), and sonicated (setting 70%, 10 s on, 10 s off, 10 times; Q500 Sonicator, Qsonica). Cells were spun down at 15,000 rpm for 15 min at 4 °C, and lysates were incubated with HisPur™ Ni-NTA Resin (Thermo Fisher) at room temperature for 3 h. Subsequently, beads were washed twice with Buffer A, twice with Buffer A/B (1:3; Buffer B, 25 mM Tris-HCl, 20 mM imidazole, pH 6.8), and once with Buffer B, followed by boiling in 2× Laemmli sample buffer and SDS-PAGE.

Cell cycle analysis

siRNA-transfected U2OS cells were incubated with 10 μM EdU (Thermo Fisher) for 30 min before being harvested. The harvested cells were fixed with 4% paraformaldehyde at room temperature for 15 min, permeabilized by saponin-based permeabilization buffer (Thermo Fisher) for 15 min, and subjected to the EdU-click reaction using Alexa Fluor 488 picolyl azide and the click-iT Plus EdU flow cytometry assay kit (Thermo Fisher) according to the manufacturer's protocol. Cells were washed once and resuspended with 200 μg/ml of PureLink™ RNase A and eBioscience™ 7-AAD viability staining solution (Thermo Fisher). After 30 min of incubation at 37 °C, cells were analyzed with the Attune NxT acoustic focusing cytometer and the Attune NxT software version 2.7 (Thermo Fisher).

RT-quantitative PCR

RNA was isolated using TRIzol (Invitrogen) and chloroform (Sigma). cDNA synthesis was performed using a high-capacity cDNA reverse transcription kit (Applied Biosystems) according to the manufacturer's protocols. Real-time quantitative PCR was performed using Fast SYBR Green Master Mix (Applied Biosystems) and a StepOnePlus Real-Time PCR system (Applied Biosystems). Glyceraldehyde-3-phosphate dehydrogenase mRNA levels were used as a control for normalization. The following primers were used for cDNA amplification: *EP300* forward, 5′-GATGACCCTTCCCAGCCTCAAA-3′; *EP300* reverse, 5′-*GCCAGATGATCTCATGGTGAAGG*-3′; *CBP* forward 5′-AGTAACGGCACAGCCTCTCAGT-3′; *CBP* reverse 5′-CCTGTCGATACAGTGCTTCTAGG-3′.

Statistical analysis

p Values for statistical analyses were obtained using the Student's *t* test (Prism 8, GraphPad). Unpaired *t*-tests were performed with a 95% confidence interval, using two-tailed *p* values, unless stated otherwise.

Acknowledgments—We thank the members of the Kim laboratory for helpful discussions and comments. We thank Dr. Sharon Cantor for kindly providing plasmids.

Author contributions—B. N. and H. K. conceptualization; B. N., A. K., and H. K. investigation; B. N., A. K., and H. K. validation; H. K. supervision; H. K. writing-original draft; B. N., A. K., and H. K. writing-review and editing; H. K. funding acquisition.

Funding and additional information—This work was supported by the National Institutes of Health Grant CA218132 and American Cancer Society Grant RSG-18-037-01-DMC (to H. K.). The content is solely the responsibility of the authors and does not necessarily represent the official views of the National Institutes of Health.

Conflict of interest— The authors declare that they have no conflicts of interest with the contents of this article.

Abbreviations—The abbreviations used are: FA, Fanconi anemia; ICL, interstrand cross-links; FAAP, FA-associated protein; CPD, Cdc4 phosphodegron; KAT, lysine acetyltransferases; HDAC, histone deacetylase; CBP, CREB-binding protein; TSA, trichostatin A; Ni-NTA, nickel-nitrilotriacetic acid; CHX, cycloheximide; PE, phycoerythrin; EGFP, enhanced green fluorescent protein; MMC, mitomycin C; EdU, ethynyl-2′-deoxyuridine; DDR, DNA damage response; PCNA, proliferating cell nuclear antigen; EV, empty vector; Z, benzyloxycarbonyl; GST, glutathione *S*-transferase; Ub, ubiquitin.

References

1. Ceccaldi, R., Sarangi, P., and D'Andrea, A. D. (2016) The Fanconi anaemia pathway: new players and new functions. *Nat. Rev. Mol. Cell Biol.* **17,** 337–349 CrossRef Medline
2. Kottemann, M. C., and Smogorzewska, A. (2013) Fanconi anaemia and the repair of Watson and Crick DNA crosslinks. *Nature* **493,** 356–363 CrossRef Medline
3. Kee, Y., and D'Andrea, A. D. (2012) Molecular pathogenesis and clinical management of Fanconi anemia. *J. Clin. Invest.* **122,** 3799–3806 CrossRef Medline
4. Niraj, J., Färkkilä, A., and D'Andrea, A. D. (2019) The Fanconi anemia pathway in cancer. *Annu. Rev. Cancer Biol.* **3,** 457–478 CrossRef Medline
5. Kim, H., and D'Andrea, A. D. (2012) Regulation of DNA cross-link repair by the Fanconi anemia/BRCA pathway. *Genes Dev.* **26,** 1393–1408 CrossRef Medline
6. Garcia-Higuera, I., Taniguchi, T., Ganesan, S., Meyn, M. S., Timmers, C., Hejna, J., Grompe, M., and D'Andrea, A. D. (2001) Interaction of the Fanconi anemia proteins and BRCA1 in a common pathway. *Mol. Cell* **7,** 249–262 CrossRef

7. Clauson, C., Scharer, O. D., and Niedernhofer, L. (2013) Advances in understanding the complex mechanisms of DNA interstrand cross-link repair. *Cold Spring Harb. Perspect. Med.* **3,** a012732 CrossRef
8. Knipscheer, P., Räschle, M., Smogorzewska, A., Enoiu, M., Ho, T. V., Schärer, O. D., Elledge, S. J., and Walter, J. C. (2009) The Fanconi anemia pathway promotes replication-dependent DNA interstrand cross-link repair. *Science* **326,** 1698–1701 CrossRef Medline
9. Klein Douwel, D., Boonen, R. A., Long, D. T., Szypowska, A. A., Räschle, M., Walter, J. C., and Knipscheer, P. (2014) XPF-ERCC1 acts in unhooking DNA interstrand crosslinks in cooperation with FANCD2 and FANCP/SLX4. *Mol. Cell* **54,** 460–471 CrossRef Medline
10. Budzowska, M., Graham, T. G., Sobeck, A., Waga, S., and Walter, J. C. (2015) Regulation of the Rev1-pol ζ complex during bypass of a DNA interstrand cross-link. *EMBO J.* **34,** 1971–1985 CrossRef Medline
11. Walden, H., and Deans, A. J. (2014) The Fanconi anemia DNA repair pathway: structural and functional insights into a complex disorder. *Annu. Rev. Biophys.* **43,** 257–278 CrossRef Medline
12. Huang, Y., Leung, J. W., Lowery, M., Matsushita, N., Wang, Y., Shen, X., Huong, D., Takata, M., Chen, J., and Li, L. (2014) Modularized functions of the Fanconi anemia core complex. *Cell Rep.* **7,** 1849–1857 CrossRef Medline
13. Rajendra, E., Oestergaard, V. H., Langevin, F., Wang, M., Dornan, G. L., Patel, K. J., and Passmore, L. A. (2014) The genetic and biochemical basis of FANCD2 monoubiquitination. *Mol. Cell* **54,** 858–869 CrossRef Medline
14. Huang, M., Kim, J. M., Shiotani, B., Yang, K., Zou, L., and D'Andrea, A. D. (2010) The FANCM/FAAP24 complex is required for the DNA interstrand crosslink-induced checkpoint response. *Mol. Cell* **39,** 259–268 CrossRef Medline
15. Singh, T. R., Saro, D., Ali, A. M., Zheng, X. F., Du, C. H., Killen, M. W., Sachpatzidis, A., Wahengbam, K., Pierce, A. J., Xiong, Y., Sung, P., and Meetei, A. R. (2010) MHF1-MHF2, a histone-fold-containing protein complex, participates in the Fanconi anemia pathway via FANCM. *Mol. Cell* **37,** 879–886 CrossRef Medline
16. Shakeel, S., Rajendra, E., Alcón, P., O'Reilly, F., Chorev, D. S., Maslen, S., Degliesposti, G., Russo, C. J., He, S., Hill, C. H., Skehel, J. M., Scheres, S. H. W., Patel, K. J., Rappsilber, J., Robinson, C. V., *et al.* (2019) Structure of the Fanconi anaemia monoubiquitin ligase complex. *Nature* **575,** 234–237 CrossRef
17. Swuec, P., Renault, L., Borg, A., Shah, F., Murphy, V. J., van Twest, S., Snijders, A. P., Deans, A. J., and Costa, A. (2017) The FA core complex contains a homo-dimeric catalytic module for the symmetric mono-ubiquitination of FANCI-FANCD2. *Cell Rep.* **18,** 611–623 CrossRef Medline
18. Kim, H., Yang, K., Dejsuphong, D., and D'Andrea, A. D. (2012) Regulation of Rev1 by the Fanconi anemia core complex. *Nat. Struct. Mol. Biol.* **19,** 164–170 CrossRef Medline
19. Ali, A. M., Pradhan, A., Singh, T. R., Du, C., Li, J., Wahengbam, K., Grassman, E., Auerbach, A. D., Pang, Q., and Meetei, A. R. (2012) FAAP20: a novel ubiquitin-binding FA nuclear core-complex protein required for functional integrity of the FA-BRCA DNA repair pathway. *Blood* **119,** 3285–3294 CrossRef Medline
20. Leung, J. W., Wang, Y., Fong, K. W., Huen, M. S., Li, L., and Chen, J. (2012) Fanconi anemia (FA) binding protein FAAP20 stabilizes FA complementation group A (FANCA) and participates in interstrand cross-link repair. *Proc. Natl. Acad. Sci. U.S.A.* **109,** 4491–4496 CrossRef Medline
21. Xie, J., Kim, H., Moreau, L. A., Puhalla, S., Garber, J., Al Abo, M., Takeda, S., and D'Andrea, A. D. (2015) RNF4-mediated polyubiquitination regulates the Fanconi anemia/BRCA pathway. *J. Clin. Invest.* **125,** 1523–1532 CrossRef Medline
22. Wang, J., Jo, U., Joo, S. Y., and Kim, H. (2016) FBW7 regulates DNA interstrand cross-link repair by modulating FAAP20 degradation. *Oncotarget* **7,** 35724–35740 CrossRef Medline
23. Wang, J., Chan, B., Tong, M., Paung, Y., Jo, U., Martin, D., Seeliger, M., Haley, J., and Kim, H. (2019) Prolyl isomerization of FAAP20 catalyzed by PIN1 regulates the Fanconi anemia pathway. *PLoS Genet.* **15,** e1007983 CrossRef Medline
24. Jo, U., and Kim, H. (2015) Exploiting the Fanconi anemia pathway for targeted anti-cancer therapy. *Mol. Cells* **38,** 669–676 CrossRef Medline
25. Li, A., Xue, Y., Jin, C., Wang, M., and Yao, X. (2006) Prediction of *N*ϵ-acetylation on internal lysines implemented in Bayesian discriminant method. *Biochem. Biophys. Res. Commun.* **350,** 818–824 CrossRef Medline
26. Elia, A. E., Boardman, A. P., Wang, D. C., Huttlin, E. L., Everley, R. A., Dephoure, N., Zhou, C., Koren, I., Gygi, S. P., and Elledge, S. J. (2015) Quantitative proteomic atlas of ubiquitination and acetylation in the DNA damage response. *Mol. Cell* **59,** 867–881 CrossRef Medline
27. Drazic, A., Myklebust, L. M., Ree, R., and Arnesen, T. (2016) The world of protein acetylation. *Biochim. Biophys. Acta* **1864,** 1372–1401 CrossRef Medline
28. Glozak, M. A., Sengupta, N., Zhang, X., and Seto, E. (2005) Acetylation and deacetylation of non-histone proteins. *Gene* **363,** 15–23 CrossRef Medline
29. Allis, C. D., Berger, S. L., Cote, J., Dent, S., Jenuwien, T., Kouzarides, T., Pillus, L., Reinberg, D., Shi, Y., Shiekhattar, R., Shilatifard, A., Workman, J., and Zhang, Y. (2007) New nomenclature for chromatin-modifying enzymes. *Cell* **131,** 633–636 CrossRef Medline
30. Dutto, I., Scalera, C., and Prosperi, E. (2018) CREBBP and p300 lysine acetyl transferases in the DNA damage response. *Cell. Mol. Life Sci.* **75,** 1325–1338 CrossRef Medline
31. Fauquier, L., Azzag, K., Parra, M. A. M., Quillien, A., Boulet, M., Diouf, S., Carnac, G., Waltzer, L., Gronemeyer, H., and Vandel, L. (2018) CBP and P300 regulate distinct gene networks required for human primary myoblast differentiation and muscle integrity. *Sci. Rep.* **8,** 12629 CrossRef Medline
32. Gallinari, P., Di Marco, S., Jones, P., Pallaoro, M., and Steinkühler, C. (2007) HDACs, histone deacetylation and gene transcription: from molecular biology to cancer therapeutics. *Cell Res.* **17,** 195–211 CrossRef Medline
33. Xie, J., Peng, M., Guillemette, S., Quan, S., Maniatis, S., Wu, Y., Venkatesh, A., Shaffer, S. A., Brosh, R. M., Jr., and Cantor, S. B. (2012) FANCJ/BACH1 acetylation at lysine 1249 regulates the DNA damage response. *PLoS Genet.* **8,** e1002786 CrossRef Medline
34. Delvecchio, M., Gaucher, J., Aguilar-Gurrieri, C., Ortega, E., and Panne, D. (2013) Structure of the p300 catalytic core and implications for chromatin targeting and HAT regulation. *Nat. Struct. Mol. Biol.* **20,** 1040–1046 CrossRef Medline
35. Wang, F., Marshall, C. B., and Ikura, M. (2013) Transcriptional/epigenetic regulator CBP/p300 in tumorigenesis: structural and functional versatility in target recognition. *Cell Mol. Life Sci.* **70,** 3989–4008 CrossRef Medline
36. Megee, P. C., Morgan, B. A., Mittman, B. A., and Smith, M. M. (1990) Genetic analysis of histone H4: essential role of lysines subject to reversible acetylation. *Science* **247,** 841–845 CrossRef Medline
37. Zhang, W., Bone, J. R., Edmondson, D. G., Turner, B. M., and Roth, S. Y. (1998) Essential and redundant functions of histone acetylation revealed by mutation of target lysines and loss of the Gcn5p acetyltransferase. *EMBO J.* **17,** 3155–3167 CrossRef Medline
38. Wojtaszek, J. L., Wang, S., Kim, H., Wu, Q., D'Andrea, A. D., and Zhou, P. (2014) Ubiquitin recognition by FAAP20 expands the complex interface beyond the canonical UBZ domain. *Nucleic Acids Res.* **42,** 13997–14005 CrossRef Medline
39. Yen, H. C., Xu, Q., Chou, D. M., Zhao, Z., and Elledge, S. J. (2008) Global protein stability profiling in mammalian cells. *Science* **322,** 918–923 CrossRef Medline
40. Grönroos, E., Hellman, U., Heldin, C. H., and Ericsson, J. (2002) Control of Smad7 stability by competition between acetylation and ubiquitination. *Mol. Cell* **10,** 483–493 CrossRef Medline
41. Levran, O., Diotti, R., Pujara, K., Batish, S. D., Hanenberg, H., and Auerbach, A. D. (2005) Spectrum of sequence variations in the FANCA gene: an International Fanconi Anemia Registry (IFAR) study. *Hum. Mutat.* **25,** 142–149 CrossRef Medline
42. Singh, T. R., Ali, A. M., Paramasivam, M., Pradhan, A., Wahengbam, K., Seidman, M. M., and Meetei, A. R. (2013) ATR-dependent phosphorylation of FANCM at serine 1045 is essential for FANCM functions. *Cancer Res.* **73,** 4300–4310 CrossRef Medline
43. Collins, N. B., Wilson, J. B., Bush, T., Thomashevski, A., Roberts, K. J., Jones, N. J., and Kupfer, G. M. (2009) ATR-dependent phosphorylation of

FANCA on serine 1449 after DNA damage is important for FA pathway function. *Blood* **113,** 2181–2190 CrossRef Medline
44. Wang, X., Kennedy, R. D., Ray, K., Stuckert, P., Ellenberger, T., and D'Andrea, A. D. (2007) Chk1-mediated phosphorylation of FANCE is required for the Fanconi anemia/BRCA pathway. *Mol. Cell. Biol.* **27,** 3098–3108 CrossRef Medline
45. Ho, G. P., Margossian, S., Taniguchi, T., and D'Andrea, A. D. (2006) Phosphorylation of FANCD2 on two novel sites is required for mitomycin C resistance. *Mol. Cell. Biol.* **26,** 7005–7015 CrossRef Medline
46. Ishiai, M., Kitao, H., Smogorzewska, A., Tomida, J., Kinomura, A., Uchida, E., Saberi, A., Kinoshita, E., Kinoshita-Kikuta, E., Koike, T., Tashiro, S., Elledge, S. J., and Takata, M. (2008) FANCI phosphorylation functions as a molecular switch to turn on the Fanconi anemia pathway. *Nat. Struct. Mol. Biol.* **15,** 1138–1146 CrossRef Medline
47. Chen, Y. H., Jones, M. J., Yin, Y., Crist, S. B., Colnaghi, L., Sims, R. J., 3rd, Rothenberg, E., Jallepalli, P. V., and Huang, T. T. (2015) ATR-mediated phosphorylation of FANCI regulates dormant origin firing in response to replication stress. *Mol. Cell* **58,** 323–338 CrossRef Medline
48. Kee, Y., Kim, J. M., D'Andrea, A. D., and D'Andrea, A. (2009) Regulated degradation of FANCM in the Fanconi anemia pathway during mitosis. *Genes Dev.* **23,** 555–560 CrossRef Medline
49. Gibbs-Seymour, I., Oka, Y., Rajendra, E., Weinert, B. T., Passmore, L. A., Patel, K. J., Olsen, J. V., Choudhary, C., Bekker-Jensen, S., and Mailand, N. (2015) Ubiquitin-SUMO circuitry controls activated fanconi anemia ID complex dosage in response to DNA damage. *Mol. Cell* **57,** 150–164 CrossRef Medline
50. Iyer, N. G., Özdag, H., and Caldas, C. (2004) p300/CBP and cancer. *Oncogene* **23,** 4225–4231 CrossRef Medline
51. Dutta, R., Tiu, B., and Sakamoto, K. M. (2016) CBP/p300 acetyltransferase activity in hematologic malignancies. *Mol. Genet. Metab.* **119,** 37–43 CrossRef Medline
52. Giles, R. H., Peters, D. J., and Breuning, M. H. (1998) Conjunction dysfunction: CBP/p300 in human disease. *Trends Genet.* **14,** 178–183 CrossRef Medline
53. Liszczak, G., Diehl, K. L., Dann, G. P., and Muir, T. W. (2018) Acetylation blocks DNA damage-induced chromatin ADP-ribosylation. *Nat. Chem. Biol.* **14,** 837–840 CrossRef Medline
54. Cazzalini, O., Sommatis, S., Tillhon, M., Dutto, I., Bachi, A., Rapp, A., Nardo, T., Scovassi, A. I., Necchi, D., Cardoso, M. C., Stivala, L. A., and Prosperi, E. (2014) CBP and p300 acetylate PCNA to link its degradation with nucleotide excision repair synthesis. *Nucleic Acids Res.* **42,** 8433–8448 CrossRef Medline
55. Balakrishnan, L., Stewart, J., Polaczek, P., Campbell, J. L., and Bambara, R. A. (2010) Acetylation of Dna2 endonuclease/helicase and flap endonuclease 1 by p300 promotes DNA stability by creating long flap intermediates. *J. Biol. Chem.* **285,** 4398–4404 CrossRef Medline
56. Dietschy, T., Shevelev, I., Pena-Diaz, J., Hühn, D., Kuenzle, S., Mak, R., Miah, M. F., Hess, D., Fey, M., Hottiger, M. O., Janscak, P., and Stagljar, I. (2009) p300-mediated acetylation of the Rothmund-Thomson-syndrome gene product RECQL4 regulates its subcellular localization. *J. Cell Sci.* **122,** 1258–1267 CrossRef Medline
57. Chen, C. S., Wang, Y. C., Yang, H. C., Huang, P. H., Kulp, S. K., Yang, C. C., Lu, Y. S., Matsuyama, S., Chen, C. Y., and Chen, C. S. (2007) Histone deacetylase inhibitors sensitize prostate cancer cells to agents that produce DNA double-strand breaks by targeting Ku70 acetylation. *Cancer Res.* **67,** 5318–5327 CrossRef Medline
58. Cohen, H. Y., Lavu, S., Bitterman, K. J., Hekking, B., Imahiyerobo, T. A., Miller, C., Frye, R., Ploegh, H., Kessler, B. M., and Sinclair, D. A. (2004) Acetylation of the C terminus of Ku70 by CBP and PCAF controls Bax-mediated apoptosis. *Mol. Cell* **13,** 627–638 CrossRef
59. Hasan, S., Hassa, P. O., Imhof, R., and Hottiger, M. O. (2001) Transcription coactivator p300 binds PCNA and may have a role in DNA repair synthesis. *Nature* **410,** 387–391 CrossRef Medline
60. Piekna-Przybylska, D., Bambara, R. A., and Balakrishnan, L. (2016) Acetylation regulates DNA repair mechanisms in human cells. *Cell Cycle* **15,** 1506–1517 CrossRef Medline
61. Jang, E. R., Choi, J. D., and Lee, J. S. (2011) Acetyltransferase p300 regulates NBS1-mediated DNA damage response. *FEBS Lett.* **585,** 47–52 CrossRef Medline
62. Stauffer, D., Chang, B., Huang, J., Dunn, A., and Thayer, M. (2007) p300/CREB-binding protein interacts with ATR and is required for the DNA replication checkpoint. *J. Biol. Chem.* **282,** 9678–9687 CrossRef Medline